

Anti-corrosive Properties of New Eco-friendly Dimethylamino Compounds on C- steel Corrosion in 2 M HCl

A.M. Eldesoky¹, M.A. Diab^{2,*}, A.Z. El-Sonbati² and S.F.Salam²

¹Engineering Chemistry Department, High Institute of Engineering & Technology (New Damietta), Egypt and Al-Qunfudah Center for Scientific Research (QCSR), Chemistry Department, Al-Qunfudah University College, Umm Al-Qura University, KSA.

²Chemistry Department, Faculty of Science, Damietta University, Damietta 34517, Egypt.

*E-mail: m.adiab@yahoo.com

Received: 29 January 2017 / Accepted: 11 April 2017 / Published: 12 April 2017

The inhibitive effect of new eco-friendly dimethylamino compounds, named (2E,4E)-5-(4-(Dimethylamino)phenyl)-1-(pyridin-2-yl)penta-2,4-dien-1-one (Compound (I)) and (E)-1-(Anthracen-10-yl)-3-(4-(dimethylamino)phenyl)prop-2-en-1-one (Compound (II)) versus CS and its adsorption habit were obtained in 2 M HCl solution utilized Weight loss, TP, (EIS) and (EFM) techniques. The outcome obtained from IE improve with the raising the inhibitor dose. The %IE orders of organic compound are follow: Compound (II) > Compound (I). Kinetic activation parameters such as activation energy, entropy and enthalpy of activation were obtained from the influence of temperature on inhibition and corrosion. The types of new eco-friendly dimethylamino compounds are mixed kind inhibitor whose adsorption found by isotherm Temkin. EIS diagrams show that adsorption of new eco-friendly dimethylamino compounds increases the transfer resistance and decrease the capacitance of interface metal/solution. The morphology of inhibited CS was evaluated by SEM and EDX. Relation among calculations of quantum chemical and protection efficiency of the investigated assembled is confirmed by utilized the Density Functional Theory (DFT). Molecular docking was utilized to predict the binding among new eco-friendly dimethylamino compounds and the receptor of breast cancer mutant 3hb5-oxidoreductase.

Keywords: Eco-friendly, Adsorption, C-steel, SEM–EDX, Molecular docking.

1. INTRODUCTION

Acid solutions are widely used in industry, such as acid pickling of iron and steel, chemical cleaning and processing, ore production and oil well acidification [1–3]. The problems arising from acid corrosion required the development of various corrosion control techniques among which the application of chemical inhibitors has been acknowledged as most economical method for preventing

acid corrosion [4–9]. Many organics, such as quaternary ammonium salts, acetylenic alcohol, and heterocyclic compounds are widely used as inhibitors in various industries. The organic molecules adsorb on the metal surface through hetero atom, such as nitrogen, oxygen and sulfur, blocking the active sites and generating a physical barrier to reduce the transport of corrosive species to the metal surface [10–16]. Other researches revealed that the adsorption is influenced not only by the nature and surface charge of the metal, but also by the chemical structure of inhibitors. Among these organic compounds, heterocyclic substances containing nitrogen atoms, such as 4-aminoantipyrine compounds are considered to be excellent corrosion inhibitors in combating acidic corrosion due to high inhibition efficiency, good thermal stability and lack of irritating odor for many metals and alloys in various aggressive media [17–22]. Therefore, the develop of novel modified inhibitors containing 4-aminoantipyrine heterocyclic ring and the study of the relations between the chemical structure of inhibitors and their inhibition performances are of great importance, both from the industrial and theoretical points of view.

The aim of the present work is to investigate the effects of new eco-friendly dimethylamino compounds, named (2E,4E)-5-(4-(Dimethylamino)phenyl)-1-(pyridin-2-yl)penta-2,4-dien-1-one (Compound (I)) and (E)-1-(Anthracen-10-yl)-3-(4-(dimethylamino)phenyl)prop-2-en-1-one (Compound (II)) versus CS and its adsorption habit were done in 2 M HCl solution by Weight loss , EFM, EIS and TP technique. Thermodynamic activation parameters were evaluated from experimental data. The relationships among the inhibition performances of the investigated inhibitor in 2 M HCl and some quantum chemical parameters, such as the biggest occupied molecular orbital energy (E_{HOMO}), the lowest unoccupied molecular orbital energy (E_{LUMO}).

2. EXPERIMENTAL

2.1. Measurements

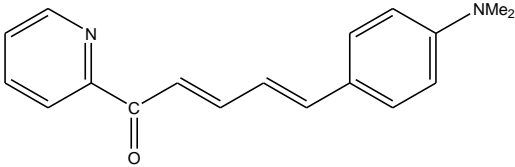
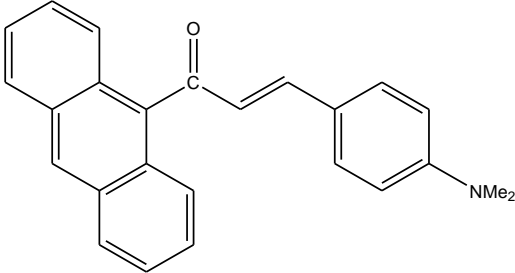
In the research simulates the actual docking process in which the ligand–protein pair-wise interaction energies are evaluated utilized Docking Server [23]. The MMFF94 Force field was for utilized energy minimization of ligand molecule utilized Docking Server. Gasteiger partial charges were appending to the compounds (I) and (II) atoms. Merged non-polar H atoms and rotatable bonds were given. Docking evaluated were occurred on compounds (I) and (II) protein model. Mostly hydrogen atoms, Kollman united atom kind charges and solvation parameters were appending with the aid of AutoDock tools [24]. Auto Dock parameter set- and distance-rely on dielectric functions were utilized in the measurement of the van der Waals and the electrostatic terms, continually.

2.2. Material and medium

CS was utilized for the corrosion calculation. Its structure (wt%) is C 0.20, Si 0.30, Mn 0.53, S 0.055, P 0.045, Fe the rest. The solution (2 M HCl) aggressive was obtaining by liquefaction of HCl

(analytical grade, 37%) with second distilled water. The new eco-friendly friendly dimethylamino compounds, named (2E,4E)-5-(4-(Dimethylamino)phenyl)-1-(pyridin-2-yl)penta-2,4-dien-1-one (Compound (I)) and (E)-1-(Anthracen-10-yl)-3-(4-(dimethylamino)phenyl)prop-2-en-1-one (Compound (II)) utilized for this paper, whose structures were shown in Table .(1) as following [25]:

Table 1. Chemical structure, name, molecular weight and molecular formula of inhibitors.

| Compound No. | Structure | Name | Mol. Wt. / M. Formula |
|--------------|--|--|---|
| (I) |  | (2E,4E)-5-(4-(Dimethylamino)phenyl)-1-(pyridin-2-yl)penta-2,4-dien-1-one | 278 / C ₁₈ H ₁₈ N ₂ O |
| (II) |  | (E)-1-(Anthracen-10-yl)-3-(4-(dimethylamino)phenyl)prop-2-en-1-one | 351 / C ₂₅ H ₂₁ NO |

2.3. Methods

2.3.1. Weigh reduction tests

The CS coins of with spacing 20 x 20 x 2 mm were pounding with grades unlike emery paper, acetone cleaning, immerse on water bi-distilled and drainage among filter papers. After perfect massing, the coins were putted in 100 ml of 2 M hydrochloric acid entity and lack of unlike dose of inhibitors. After various rinsed time, the CS coins were obtain, rinse with water bi-distilled, dried and again weighted. The value of mass reduction is obtained to measure the corrosion rate (R) in mmy^{-1} by follow (1):

$$R = (\text{mass reduction in gram} \times 8.75 \times 10^4) / \text{DAT} \quad (1)$$

Where T = exposure time in hr, A = target area in cm^2 and D = density of iron in g cm^{-3} . The protection efficiency (%IE) and (θ) were measured from (2):

$$\% \text{ IE} = 100 \times \theta = 100 \times [(R^* - R) / R^*] \quad (2)$$

Where R and R* are the rates of CS corrosion with and without inhibitor, severally.

2.3.2. Electrochemical methods

The calculations were entertained in imitative three electrodes thermostatic cell assembly by utilizing a Gamry potentiostat/galvanostat/ZRA (model PCI300/4). (SCE) as reference and platinum foil as counter electrodes, continually. The CS electrode was size 10x10 mm and was fused from first side to a copper wire utilized for linkage electrical. The electrodes were studied similar as mass reduction. The Tafel polarization (TP) diagrams were reported from -5 to 5 V at a rate of scan 1 mV S^{-1} after the state of steady is obtained (half hours).

Electrochemical impedance spectroscopy (EIS) and electrochemical frequency modulation (EFM) tests were performed utilizing the same behaviors as before with a Gamry framework system depend on ESA400. Gamry applications contain software EIS300 for EIS tests and EFM140 for EFM calculations; computer was utilized for data summation. Echem Analyst 5.5 Software was utilized for plotting, graphing and fitting value. EFM executes by utilizing two frequencies 2 and 5 Hz.

2.3.3. Energy Dispersion Spectroscopy (EDX) - Scanning electron microscopy (SEM) technique

The CS surface was carried out by putting the sample for three days inundation in 2 M HCl without and with of excellent dose of new eco-friendly dimethylamino compounds, named (2E,4E)-5-(4-(Dimethylamino)phenyl)-1-(pyridin-2-yl)penta-2,4-dien-1-one (Compound (I)) and (E)-1-(Anthracen-10-yl)-3-(4-(dimethylamino)phenyl)prop-2-en-1-one (Compound (II)), after mechanically pounding utilized unlike papers emery up to 2000 size grit. Then, after this inundation time, the coins were gently rinsed with water bi-distilled, dried and directly putted in spectrometer. The corroded C-steel were tested by utilizing diffractometer X-ray Philips (pw-1390) with Cu-tube, (SEM, JSM-T20, JOEL, Japan).

2.3.4. Theoretical Research

(Material Studio Version 4.4) Accelrys software utilized for evaluated chemical quantum data.

3. RESULTS AND DISCUSSION

3.1. Weight loss method

Figure 1 illustrated the Weight loss-time plots for C-steel corrosion in 2 M HCl attendance and lack of unlike concentrating of assembled (I) at $30 \pm 1^\circ\text{C}$. The same diagram for other compound was carried out and is doesn't give. The value record on Table 2 given that, the protection efficiency improves with reinforced in dose of inhibitor from 1×10^{-6} to 11×10^{-6} M. The best (% IE) was given at 11×10^{-6} M. The minimum (% IE) is given with compound (I), therefore %IE tends to decrease in the following order: Compound (II) > Compound (I).

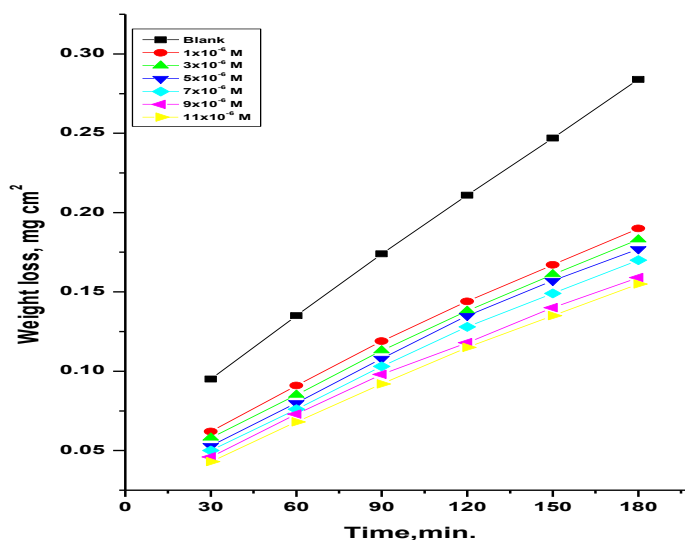


Figure 1. Time -mass reduction plots for CS liquefaction in 2 M acid without and with unlike dose of (I).

Table 2. The %IE of unlike assembled with their molar doses from mass reduction method at 60 min rinsed in acidic medium at $30 \pm 1^\circ\text{C}$.

| Conc. (M) | (%IE) | |
|---------------------|--------------|---------------|
| | Compound (I) | Compound (II) |
| 1×10^{-6} | 26.6 | 31.0 |
| 3×10^{-6} | 31.9 | 36.8 |
| 5×10^{-6} | 35.0 | 40.0 |
| 7×10^{-6} | 37.2 | 41.7 |
| 9×10^{-6} | 38.9 | 43.7 |
| 11×10^{-6} | 40.2 | 44.7 |

3.1.1. Adsorption isotherm

Its gives useful light onto mechanism of corrosion protection and the reaction among the adsorb molecules themselves and the electrode [26]. In paper, adsorption Temkin isotherm was obtained to the excellent for the outcome data and given as follow:

$$\theta = 2.303/a \log C + 2.303/a \log K_{ads} \tag{3}$$

Where C = inhibitor dose and K_{ads} = equilibrium constant of adsorption. The plot of θ against $\log C$ was linear relationship (illustrated in Figure 2). The measure K_{ads} from the intercept. Also obtained ΔG^0_{ads} :

$$\log K_{ads} = -\log 55.5 - \Delta G^0_{ads}/ 2.303RT \tag{4}$$

where data of 55.5 = water dose in mole/liter [27], R = gas constant universal and T = temperature by kelvin [28]. From Table 3, the data of K_{ads} were attendance to parallel run to the %IE

[K (II) > K (I)]. This outcome inverts the capability improvement, due to formation structural on the surface of alloy [29].

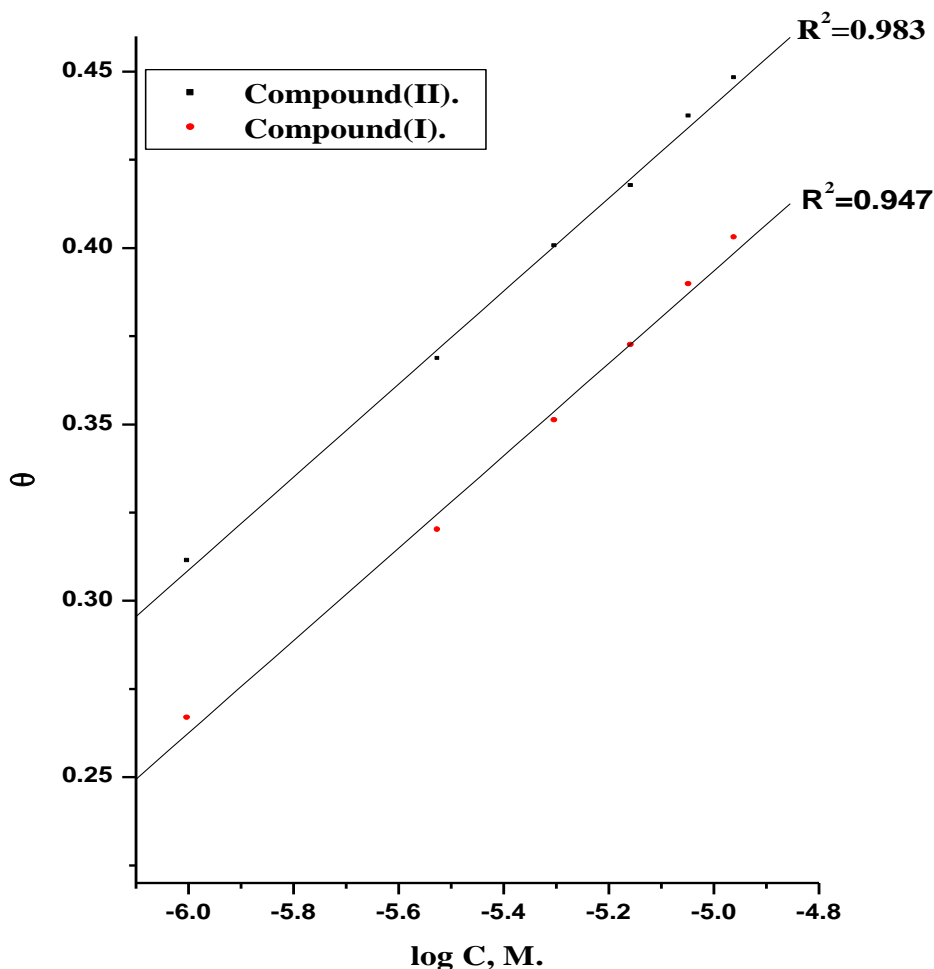


Figure 2. CS diagrams of corrosion fitting data attendance of various dose of inhibitors obeys the Temkin.

Table 3. Data from isotherm Temkin (K_{ads}), (ΔG_{ads}) and (a) for inhibitors.

| Inhibitors | Temkin | | |
|---------------|--------|-------------------|-------------------------------|
| | a | K_{ads}, M^{-1} | $-\Delta G_{ads}, kJmol^{-1}$ |
| Compound (I) | 80.19 | 1.21 | 9.76 |
| Compound (II) | 83.07 | 1.27 | 9.98 |

3.1.2. Kinetic activation parameters

The activation energies (E_a^*) for the C-steel corrosion attendance and lack of unlike dose of new eco-friendly dimethylamino compounds, named (2E,4E)-5-(4-(Dimethylamino)phenyl)-1-(pyridin-2-yl)penta-2,4-dien-1-one (Compound (I)) and (E)-1-(Anthracen-10-yl)-3-(4-

(dimethylamino)phenyl)prop-2-en-1-one (Compound (II)) were measure utilized Arrhenius-kind [30]:

$$\log k = \log A - E_a^* / 2.303RT \tag{5}$$

Where E_a^* = corrosion activation energy, k = constant rate, A = pre-exponential factor, T = absolute temperature and R = constant gas. Arrhenius plots of $\log k$ vs. $1/T$ for metal in 2 M hydrochloric acid without and with various dose of (I) is given graphically in Figure 3. The variation is a linear line. The data of E_a^* were measured from the slope of these lines and record in Table 4. The rise in E_a^* by the appending of dose of inhibitors (I, II) lead to that the energy barrier for the corrosion improve. The process whole is exactly by surface reaction, since the E_a^* is higher than 20 kJ mol^{-1} [31]. (ΔH^* , ΔS^*) for the C-steel corrosion in acidic medium was obtained by utilized the transition state equation (6):

$$k = (TR / Nh) e^{(\Delta S^*/R)} e^{(-\Delta H^*/RT)} \tag{6}$$

Where h = constant Planck's, N = Avogadro's number,. A plot of $1/T$ against $\log k/T$ also gave linier lines as obtain in Figure 4 for C-steel in hydrochloric acid with and uninhibited dose (I). The intercept $= \log RT/Nh + (\Delta S^*/2.303R)$ and the lines slopes $= -\Delta H^*/2.303R$, ΔH^* and ΔS^* were measured and record in Table 4.

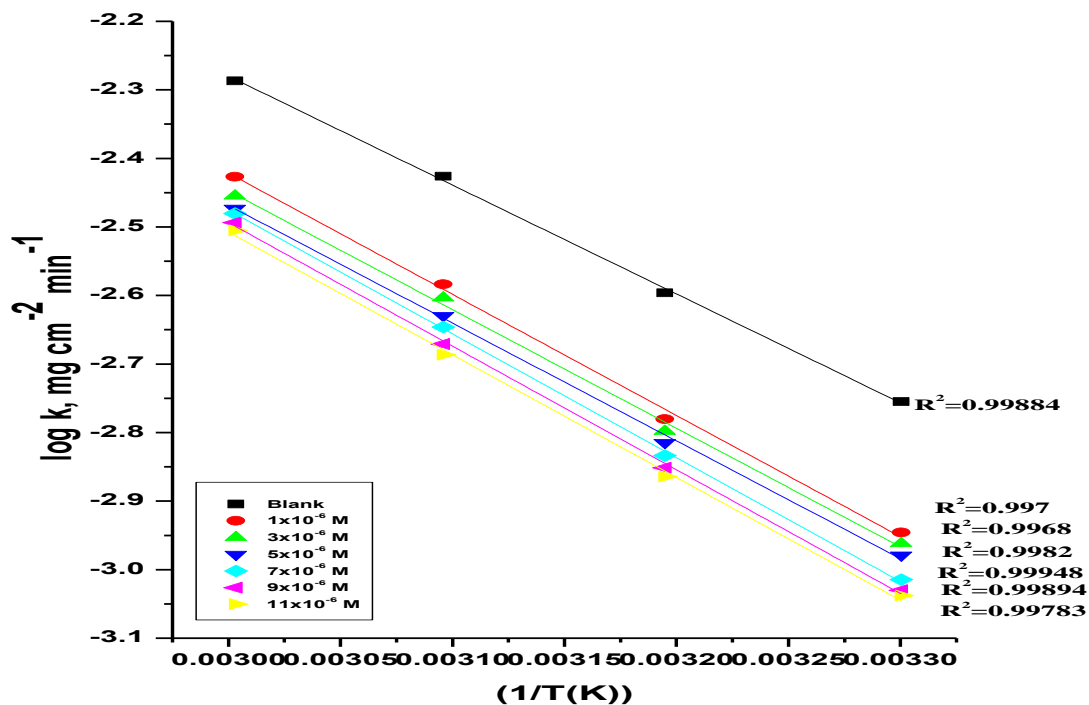


Figure 3. 1/T vs.log k for CS attendance and lack of various dose of (I)

The outcome data, the attendance of the tested composite rise values of E_a^* and consequently lower the C-steel corrosion rate. These outcomes given that these composite tested play as inhibitors through improve E_a^* of CS liquefaction by making a barrier to charge transfer by their adsorption on alloy surface. The sign +ve of the ΔH^* evaluated the endothermic type for CS liquefaction.

All data of E_a^* are biggest than the analogous data of ΔH^* lead to that the corrosion process must contain a gaseous, uncomplicated evolution hydrogen reaction, associated with a lower in the total volume of reaction [32]. The data of ΔS^* attendance and lack of the tested assembled are higher and – ve sign; i.e. the activated complex in the rate-determining step performance association rather than dissociation step, meaning that a lower in disordering obtain on going to the activated complex [33, 34].

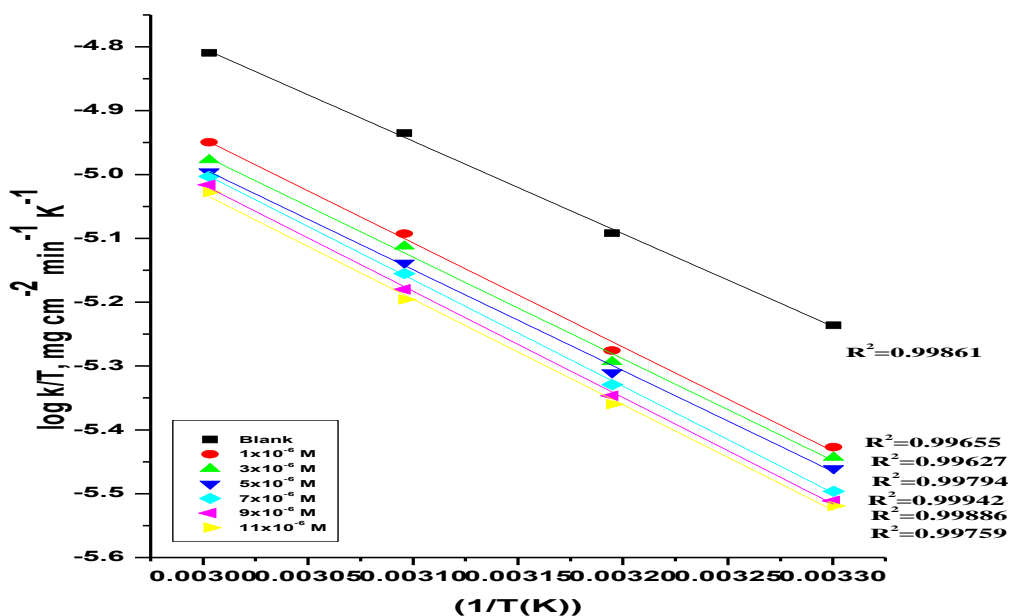


Figure 4. Transition state plots for CS attendance and lack unlike concentration of inhibitor (I).

Table 4. Kinetic activation parameters for the liquefaction of CS with and lack of unlike dose of investigated organic compounds (I) and (II) .

| Inhibitor | Conc., M | E_a^* , kJ mol ⁻¹ | ΔH^* , kJ mol ⁻¹ | $-\Delta S^*$, J mol ⁻¹ K ⁻¹ |
|---------------|---------------------|--------------------------------|-------------------------------------|---|
| Compound (I) | Blank | 29.87 | 26.98 | 205.89 |
| | 1x10 ⁻⁶ | 30.96 | 29.43 | 204.67 |
| | 3x10 ⁻⁶ | 31.04 | 29.45 | 203.32 |
| | 5 x10 ⁻⁶ | 31.65 | 29.89 | 203.10 |
| | 7x10 ⁻⁶ | 31.87 | 31.01 | 202.07 |
| | 9x10 ⁻⁶ | 32.54 | 31.77 | 198.64 |
| | 11x10 ⁻⁶ | 33.11 | 31.87 | 197.68 |
| Compound (II) | 1x10 ⁻⁶ | 31.08 | 29.88 | 203.33 |
| | 3x10 ⁻⁶ | 31.87 | 30.69 | 202.66 |
| | 5 x10 ⁻⁶ | 32.06 | 31.22 | 201.45 |
| | 7x10 ⁻⁶ | 33.06 | 32.32 | 200.01 |
| | 9x10 ⁻⁶ | 33.88 | 33.08 | 198.22 |
| | 11x10 ⁻⁶ | 35.10 | 33.74 | 197.44 |

3.2. Tafel polarization methods

TP were occurred to given information relating to the kinetics of the anodic and cathodic reactions. Figure 5 give the polarization habit of CS electrode in acidic medium without and attendance of various concentrated of compound (I). Figure 5 illustrated affected both the anodic and cathodic reactions by appending of investigated new eco-friendly dimethylamino compounds, named (2E,4E)-5-(4-(Dimethylamino)phenyl)-1-(pyridin-2-yl)penta-2,4-dien-1-one (Compound (I)) and (E)-1-(Anthracen-10-yl)-3-(4-(dimethylamino)phenyl)prop-2-en-1-one (Compound (II)) and the % IE rise as the dose of inhibitor rise, but the cathodic is more protective, indication by appending of new eco-friendly dimethylamino compounds, named (2E,4E)-5-(4-(Dimethylamino)phenyl)-1-(pyridin-2-yl)penta-2,4-dien-1-one (Compound (I)) and (E)-1-(Anthracen-10-yl)-3-(4-(dimethylamino)phenyl)prop-2-en-1-one (Compound (II)) lower the anodic C-steel liquefaction and also pervent the cathodic reactions. Therefore, investigated new eco-friendly dimethylamino compounds, named (2E,4E)-5-(4-(Dimethylamino)phenyl)-1-(pyridin-2-yl)penta-2,4-dien-1-one (Compound (I)) and (E)-1-(Anthracen-10-yl)-3-(4-(dimethylamino)phenyl)prop-2-en-1-one (Compound (II)) are point as mixed inhibitors. The outcome value from Table 5 show current corrosion density decreases with presence inhibitors and rise % IE with raising the dose of inhibitor. The %IE_p was measure utilized as the following:

$$\%IE_p = 100 \times [i_{\text{corr}}^0 - i_{\text{corr}}]/i_{\text{corr}}^0 \quad (7)$$

Where, i_{corr}^0 and i_{corr} are the uninhibited and inhibited corrosion current densities, severally.

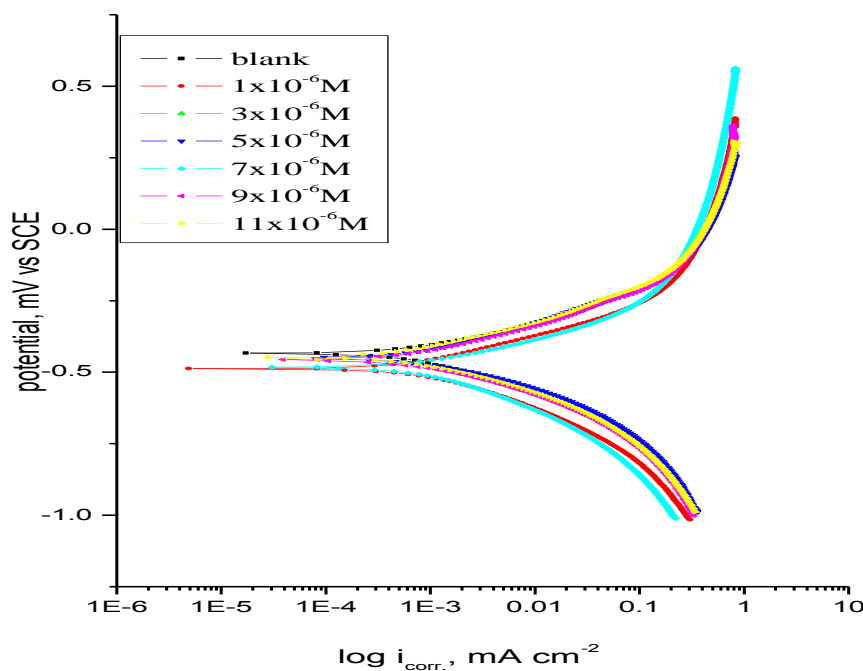


Figure 5. TP plots for the CS corrosion attendance and lack of unlike dose of compound (I).

It is illustrated from next table the adsorbed inhibitors act by plain blocking of the active center for both anodic and cathodic. In other words, the inhibitors adsorbed lower the surface area for

corrosion without impact the CS corrosion mechanism [35,36]. The protective efficiency of these composites obeys the sequence: Compound (II) > Compound (I). This succession due to free pair of electron in the alternative in the molecular structure, π electrons on aromatic nuclei, N atom and again invert, as affirm from mass reduction methods, the ability rise from (II) to inhibit 2 M hydrochloric acid compared to (I).

Table 5. parameters given from TP diagrams ($E_{\text{corr.}}$), ($i_{\text{corr.}}$), (β_a & β_c), (θ) and (% IE) for C-steel in 2 M HCl.

| | Conc., M | $i_{\text{cor}} \times 10^{-4}$ mA cm^{-2} | $-E_{\text{corr}}$ mV vs(SCE) | $\beta_a \times 10^{-3}$, mV dec^{-1} | $\beta_c \times 10^{-3}$, mV dec^{-1} | θ | % IE |
|---------------|---------------------|--|----------------------------------|--|--|----------|-------|
| | Blank | 8.23 | 436 | 106 | 144 | - | - |
| Compound (I) | 1×10^{-6} | 6.34 | 489 | 117 | 119 | 0.2296 | 22.96 |
| | 3×10^{-6} | 6.23 | 462 | 113 | 131 | 0.2430 | 24.30 |
| | 5×10^{-6} | 5.79 | 461 | 124 | 86 | 0.2964 | 29.64 |
| | 7×10^{-6} | 5.47 | 477 | 86 | 119 | 0.3353 | 33.53 |
| | 9×10^{-6} | 4.99 | 455 | 116 | 98 | 0.3936 | 39.36 |
| | 11×10^{-6} | 4.42 | 452 | 37 | 35 | 0.4629 | 46.29 |
| Compound (II) | 1×10^{-6} | 5.67 | 447 | 23 | 88 | 0.3111 | 31.11 |
| | 3×10^{-6} | 4.99 | 444 | 82 | 94 | 0.3937 | 39.37 |
| | 5×10^{-6} | 4.33 | 453 | 34 | 29 | 0.4739 | 47.39 |
| | 7×10^{-6} | 4.12 | 455 | 98 | 71 | 0.4994 | 49.94 |
| | 9×10^{-6} | 3.87 | 440 | 102 | 87 | 0.5298 | 52.98 |
| | 11×10^{-6} | 3.17 | 471 | 35 | 31 | 0.6148 | 61.48 |

3.3. EIS technique

EIS is strength test in the research of corrosion [37-41]. Figure 6 give Nyquist curve show at open-circuit potential both in attendance and lack of improving doses of investigated compound (I) at $30 \pm 1^\circ\text{C}$. The same diagram for other compound was carried out and is not shown. The rise in the area of the capacitive loop with the appending of compound (I) illustrated that a barrier stepwise forms on the C- Steel surface. The rise size of capacitive loop Figure 6 fortify, at a fixed inhibitor dose given the order: Compound (II) > Compound (I), declaring the biggest protective influence of compound (I).

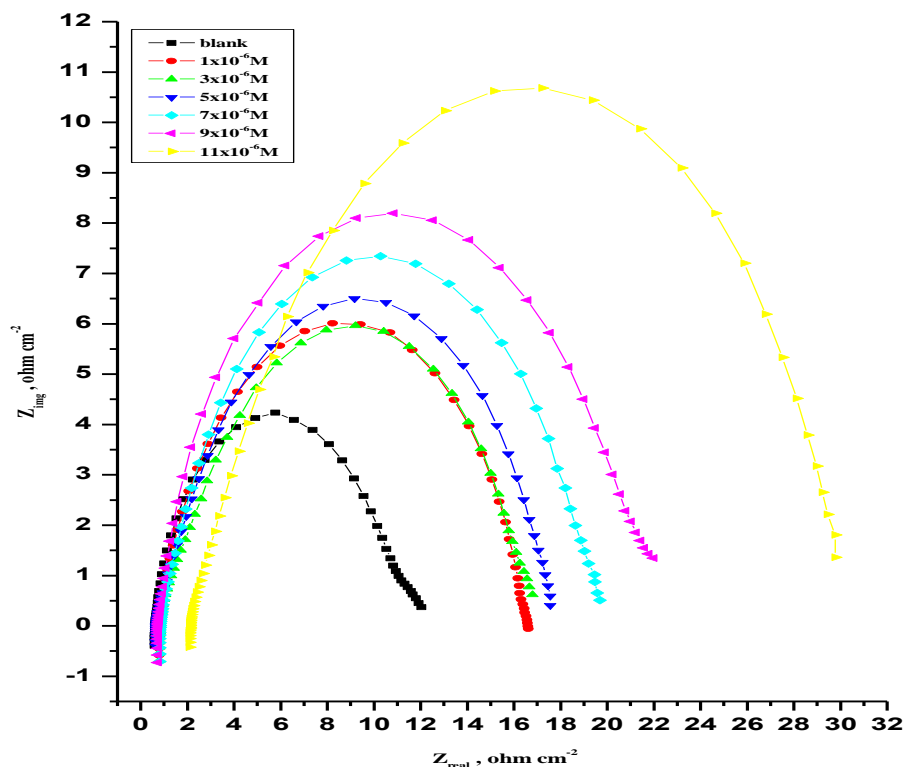


Figure 6. EIS Nyquist plots for CS surface attendance and lack of unlike dose of compound (I).

The Nyquist curves do not give semicircles perfect as hope-for from the theory of EIS. The declination from semicircle ideal was stepwise imputed to the dispersion frequency [42] Figure 7, given a single reaction charge transfer and follow well with our outcome experimental. The CPE is interfering in the circuit equivalent of a pure capacitor double layer to obtain a more correct fit [43]. The C_{dl} , is measure as equation. (8):

$$C_{dl} = Y_o \omega^{n-1} / \sin [n (\pi/2)] \tag{8}$$

Where $Y_o =$ CPE content, $\omega = 2\pi f_{max}$, $f_{max} =$ frequency of imaginary assembled of the impedance is maximal and $n =$ exactly parameter factor.

After authorization the plot of the Nyquist curve, it is noted that the diagrams nearly by a single semicircles capacitive, giving that the corrosion mechanism was widely charged-transfer command [44-46]. The mostly shape of the plots is very like for all solutions (without and with inhibitors at unlike flooding times) lead to corrosion process no change [47]. From EIS value (Table 6), we contain that the data of R_{ct} improve with improving the inhibitors dose and this given % IE higher, which in similar with the outcome mass loss. The data of R_{ct} in acidic medium rises with attendance of inhibitor. C_{dl} data are also lower to the highest extent in attendance of inhibitor and the lower in the data of CPE. The lower in CPE/ C_{dl} outcome from brought down in local dielectric constant and/or improve in the double layer thickness, lead to organic derivatives prevent the corrosion of C-steel by metal/acid adsorption [48, 49]. The % IE was measured from R_{ct} value as [50]:

$$\% IE_{EIS} = 100 \times [1 - (R_{ct}^{\circ} / R_{ct})] \tag{9}$$

i.e.; R_{ct} and R_{ct}° are the resistance charge-transfer data lack and attendance of inhibitor, continually.

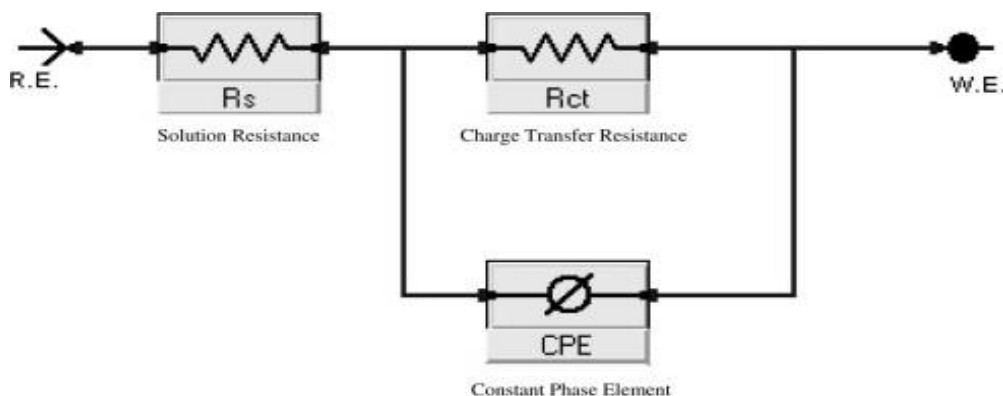


Figure 7. Equivalent circuit utilized to fit EIS data.

Table 6. parameters given by EIS method for C-steel in 2 M HCl lack and with various dose of organic compounds (I) and (II).

| Compound No. | Conc.,M | $R_s \times 10^{-1}, \Omega cm^2$ | $Y_o, \times 10^{-4} \mu\Omega^{-1}s^n$ | $n \times 10^{-1}$ | $R_{ct}, \Omega cm^2$ | $C_{dl} \times 10^{-4}, \mu F cm^{-2}$ | θ | %IE |
|---------------|---------------------|-----------------------------------|---|--------------------|-----------------------|--|----------|-------|
| Compound (I) | Blank | 6.15 | 6.41 | 8.8 | 10.74 | 9.7 | ----- | ----- |
| | 1×10^{-6} | 9.21 | 2.72 | 8.6 | 12.03 | 9.1 | 0.107 | 10.7 |
| | 3×10^{-6} | 7.51 | 1.35 | 8.1 | 12.55 | 9.0 | 0.144 | 14.4 |
| | 5×10^{-6} | 6.88 | 3.81 | 8.9 | 13.74 | 8.9 | 0.218 | 21.8 |
| | 7×10^{-6} | 7.29 | 3.21 | 8.7 | 13.78 | 8.7 | 0.221 | 22.1 |
| | 9×10^{-6} | 6.19 | 1.46 | 8.2 | 14.14 | 8.2 | 0.240 | 24.0 |
| | 11×10^{-6} | 6.13 | 1.55 | 8.3 | 14.51 | 7.7 | 0.260 | 26.0 |
| Compound (II) | 1×10^{-6} | 8.11 | 3.16 | 8.6 | 15.57 | 5.9 | 0.310 | 31.0 |
| | 3×10^{-6} | 7.89 | 1.83 | 7.5 | 16.40 | 5.0 | 0.345 | 34.5 |
| | 5×10^{-6} | 6.56 | 1.67 | 7.8 | 17.34 | 4.8 | 0.381 | 38.1 |
| | 7×10^{-6} | 8.35 | 9.41 | 8.3 | 18.97 | 3.0 | 0.434 | 43.4 |
| | 9×10^{-6} | 7.51 | 7.36 | 8.7 | 20.90 | 2.7 | 0.486 | 48.6 |
| | 11×10^{-6} | 6.23 | 2.21 | 7.5 | 29.33 | 2.3 | 0.634 | 63.4 |

3.4. EFM method

EFM is a nondestructive corrosion analysis tests that can undertake and quickly evaluated the current corrosion data without prior information of Tafel slopes. These important of EFM tests make it real candidate for corrosion online calculation [51]. The causality factors which attend as an internal examine on the exactitude of EFM caculation. The causality factors CF-2 and CF-3 are measure from the current of frequency spectrum.

Figure 8 given the EFM of CS solution with various dose of compound (I). The same plots were give for other compounds (not shown). The harmonic and intermodulation band are apparent visible and are much higher than the noise of background. EFM values were treated utilized two unlike models: perfect control diffusion of the cathodic reaction and the “activation” model. For second, a set of 3 non-linear equations had been occurs, assuming that the potential of corrosion doesn't change because the polarization of the working electrode [52].The maximum peaks were utilized to measure the (β_c and β_a), (CF-2 and CF-3) and (i_{corr}).These parameters were record in Table 7.The data for appending composite brought down i_{corr} , lead to these composite prevent the corrosion of alloy in 2 M hydrochloric acid by adsorption. The causality factors obtain under unlike tests are nearly equal to the theoretical data lead to that the calculated value are perfect and of quality best. % IE_{EFM} improve by rising the composite dose as equation (10):

$$\%IE_{EFM} = 100 \times [1 - (i_{corr} / i_{corr}^0)] \tag{10}$$

Where, i_{corr} and i_{corr}^0 are current densities lack and attendance of compsite, respectively.

The order of IE given from this tests are: Compound (II) > Compound (I).

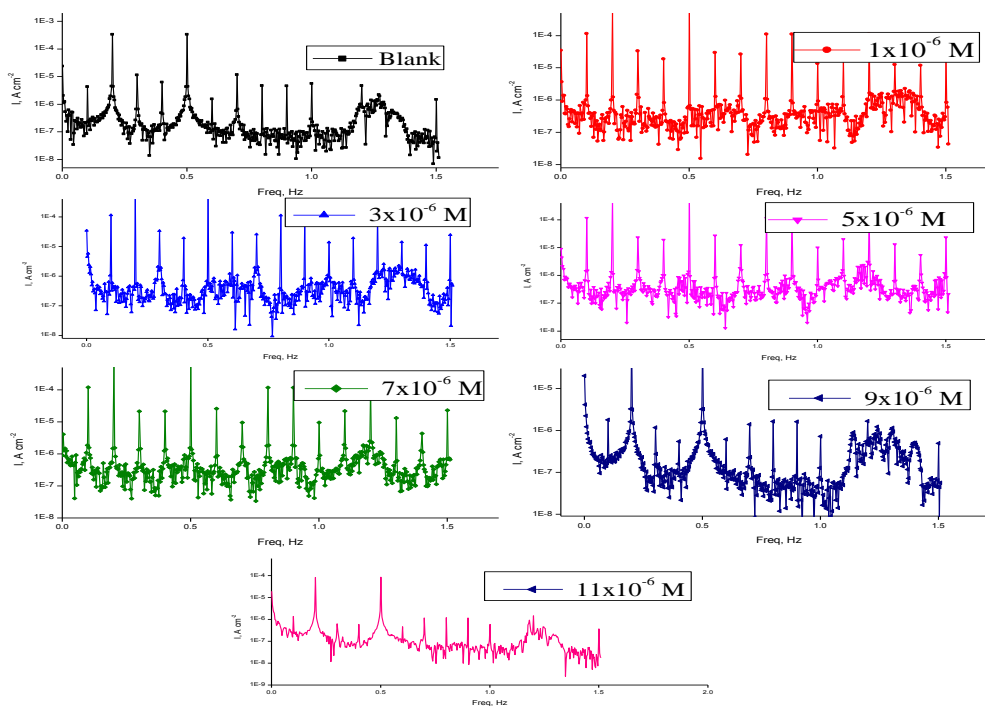


Figure 8. EFM spectra for CS attendance and lack of unlike dose of composite (I).

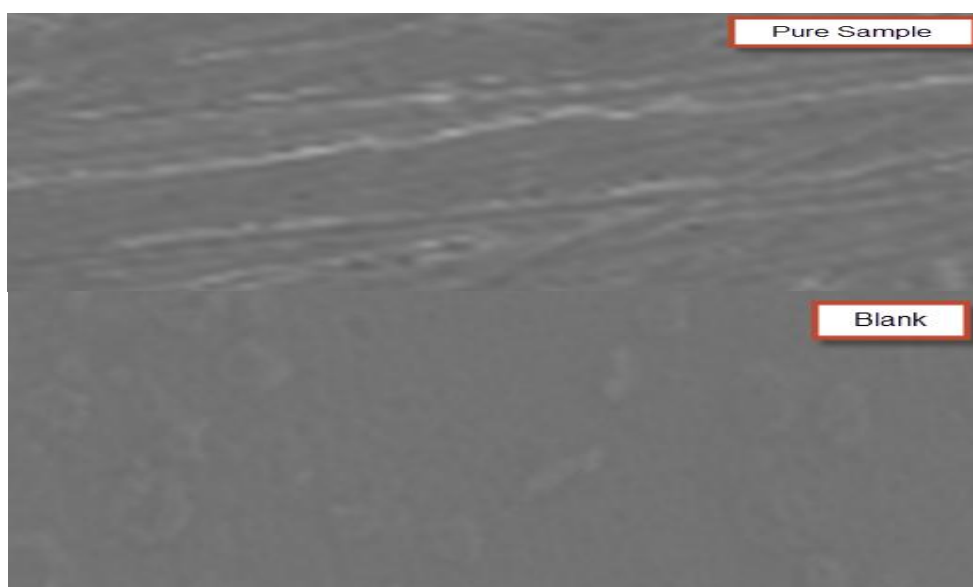
Table 7. EFM parameters obtain form CS with and lack of unlike dose of organic compounds (I) and (II).

| Compound No. | Conc., M. | i_{corr} , $\mu A cm^2$ | $\beta_a \times 10^{-3}$, $mV dec^{-1}$ | $\beta_c \times 10^{-3}$, $mV dec^{-1}$ | CF-2 | CF-3 | θ | %IE |
|--------------|--------------------|---------------------------|--|--|------|------|----------|-------|
| Compound (I) | Blank | 531.7 | 908 | 110 | 1.98 | 2.89 | - | - |
| | 1×10^{-6} | 458.4 | 752 | 834 | 2.00 | 2.95 | 0.1379 | 13.79 |

| | | | | | | | | |
|---------------|---------------------|-------|-----|-----|------|------|--------|-------|
| | 3×10^{-6} | 348.2 | 460 | 557 | 1.97 | 3.07 | 0.3451 | 34.51 |
| | 5×10^{-6} | 303.8 | 371 | 433 | 1.67 | 3.11 | 0.4286 | 42.86 |
| | 7×10^{-6} | 269.6 | 340 | 346 | 1.85 | 2.98 | 0.4929 | 49.29 |
| | 9×10^{-6} | 254.2 | 331 | 347 | 1.94 | 3.04 | 0.5219 | 52.19 |
| | 11×10^{-6} | 239.0 | 285 | 303 | 2.02 | 3.07 | 0.5505 | 55.05 |
| Compound (II) | 1×10^{-6} | 343.1 | 272 | 319 | 2.06 | 3.14 | 0.3547 | 35.47 |
| | 3×10^{-6} | 237.6 | 283 | 299 | 2.03 | 2.78 | 0.5531 | 55.31 |
| | 5×10^{-6} | 227.2 | 284 | 297 | 2.07 | 2.98 | 0.5727 | 57.27 |
| | 7×10^{-6} | 216.5 | 276 | 289 | 1.97 | 2.90 | 0.5928 | 59.28 |
| | 9×10^{-6} | 207.9 | 267 | 284 | 2.07 | 2.98 | 0.6090 | 60.90 |
| | 11×10^{-6} | 198.3 | 262 | 279 | 2.09 | 3.04 | 0.6270 | 62.70 |

3.5. (SEM) tests

Figure 9 given the micrography obtained for alloy coins in without and with 11×10^{-6} M of new eco-friendly dimethylamino compounds, named (2E,4E)-5-(4-(Dimethylamino)phenyl)-1-(pyridin-2-yl)penta-2,4-dien-1-one (Compound (I)) and (E)-1-(Anthracen-10-yl)-3-(4-(dimethylamino)phenyl)prop-2-en-1-one (Compound (II)) after exposure for 3 days inundation. C-steel surfaces suffer from severe corrosion attack in the blank sample. It is important to stress out that when the compound is attendance in the solution, the C-steel morphology is quite unlike from the preceding one, and the smoother of coins surfaces. We observed the formation of a film which is distributed in a random way on the whole surface of the C-steel, due to the adsorption of the organic (I, II) on the alloy surface merging into the passive film in order to block the active center due to attendance on the surface of CS. Or due to the inhibitor molecules reaction with the CS sites, lead to a break down in the connection among C-steel and the hydrochloric acid and sequentially prevent good inhibition influence [53, 54].



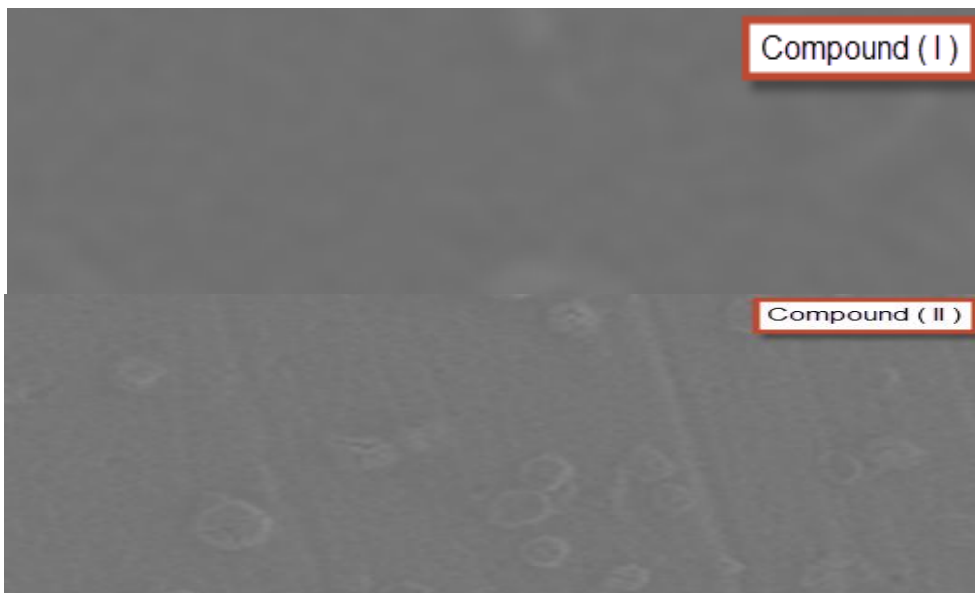
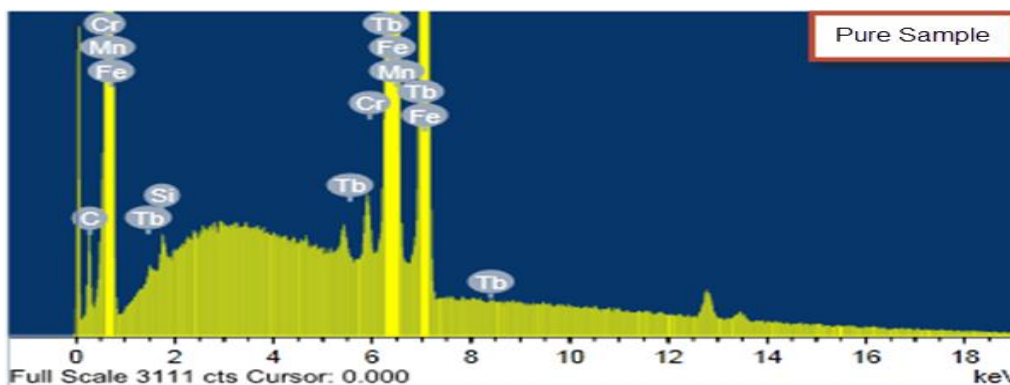


Figure 9. SEM picture of CS after rinsed for 3 days lack inhibitor and in presence of 11×10^{-6} M of dimethylamino compounds (I, II).

3.6. (EDX) tests

Its utilized to evaluated the elements attendance on the surface of C - steel and after rinsed 3 days of putted in the uninhibited and inhibited 2M acid. The EDS tests lead to only O and Fe were obtained, which had formed the passive film with only ferric oxide.

Figure 10 portrays the EDS analysis of C-steel only and attendance of 11×10^{-6} M of dimethylamino compounds (I, II).The spectra given appending lines, demonstrating the attendance of C (owing to the carbon atoms of dimethylamino compounds (I, II)). These values conducted that the C and O atoms adherent to the coins. This layer is entirely owing to the inhibitor, because the signals of C and O are lack on the alloy surface exposed to uninhibited HCl. A distribution elemental is given in Table 8.



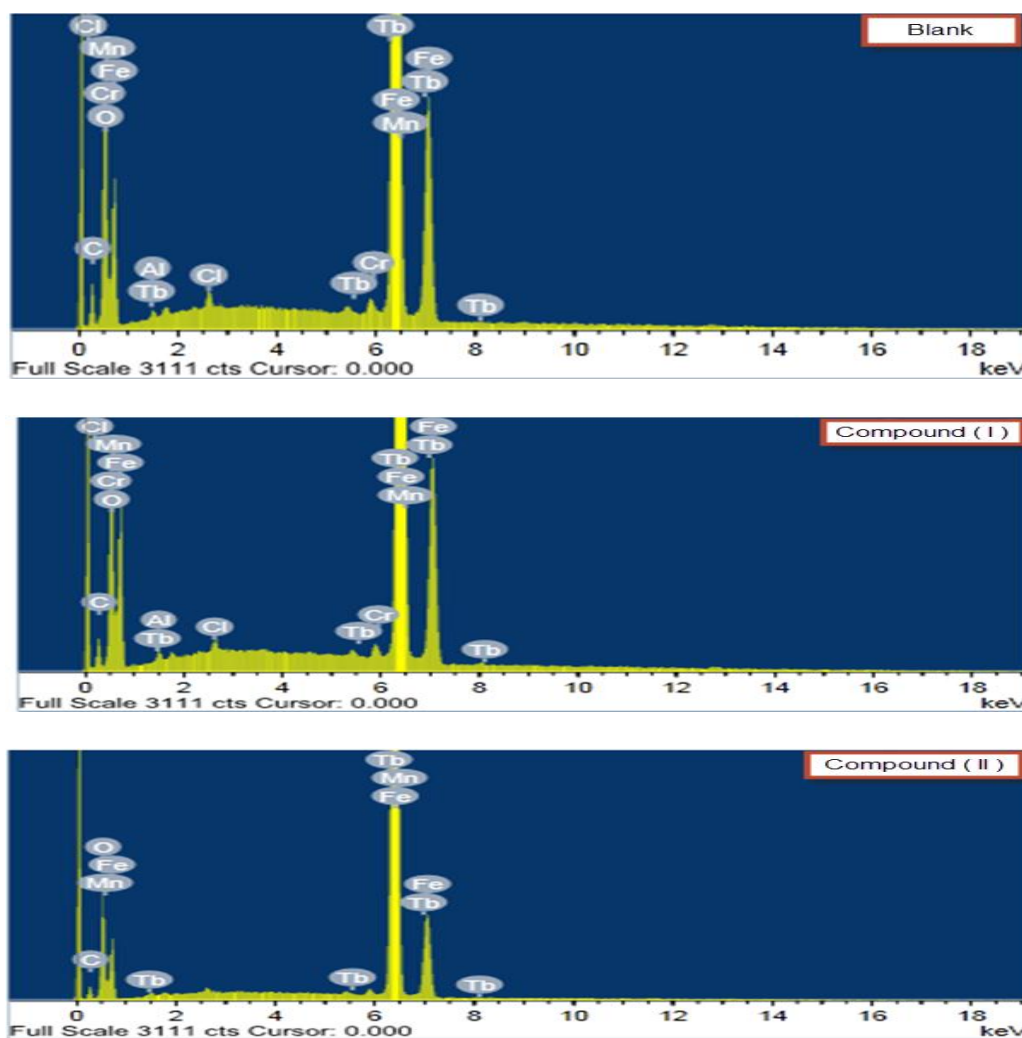


Figure 10. Analysis EDS of CS solution after rinsed for days attendance and lack of 11×10^{-6} M of dimethylamino compounds.

Table 8. (weight %) of CS after 3 days of rinsed in acidic solution attendance and lack of optimum doses of the dimethylamino compounds studied.

| (Mass %) | C | O | Al | Si | Cr | Mn | Fe | Tb | Cl |
|---------------|-------|-------|------|------|------|------|-------|------|------|
| Pure Sample | 6.78 | ---- | 0.29 | 0.28 | 0.22 | 0.47 | 87.53 | 4.43 | ---- |
| Blank | 10.99 | 21.58 | 0.30 | ---- | 0.16 | 0.34 | 62.75 | --- | 0.33 |
| Compound (I) | 8.99 | 19.45 | 0.40 | ---- | 0.17 | 0.40 | 66.78 | 3.58 | ---- |
| Compound (II) | 9.51 | 21.01 | ---- | ---- | --- | 0.45 | 66.10 | 2.93 | ---- |

3.7. Quantum theory

Figure 11 portrays the molecular orbital curves and Mulliken charges of organic (I, II). Theoretical analysis were made it for only the neutral forms, in order to obtain further insight into the outcome experimental. Data of quantum indices such as energy gap (ΔE), energy of highest occupied molecular orbitals (E_{HOMO}) and (E_{LUMO}) are given in Table 9. It has been conducted that the higher or lower -ve E_{HOMO} is related to inhibitor, the higher the trend of offering electrons to unoccupied d orbital of the metal, the improve the corrosion IE, in appending, the brought down of E_{LUMO} , the gain of electrons easier from alloy surface [55,56]. From Table 9, the ΔE given of composite (I) is decrease than (II), which improve the assumption that (II) molecule will absorb more best on CS than (I), due to easily transfer of electron among molecular orbital LUMO and HOMO which carried out due its adsorption on CS and next attendance the higher %IE.

Also the E_{HOMO} rise from compound (II) to compound (I) facilitates the adsorption and the inhibition by supporting the transport process through the adsorbed layer. The perfect inhibitors for corrosion are utilized from organic comosite who are not only offer electrons to unoccupied orbital of the alloy, but also gain electrons free from the CS [57]. From all quantum calculation parameters validate these outcome experimental.

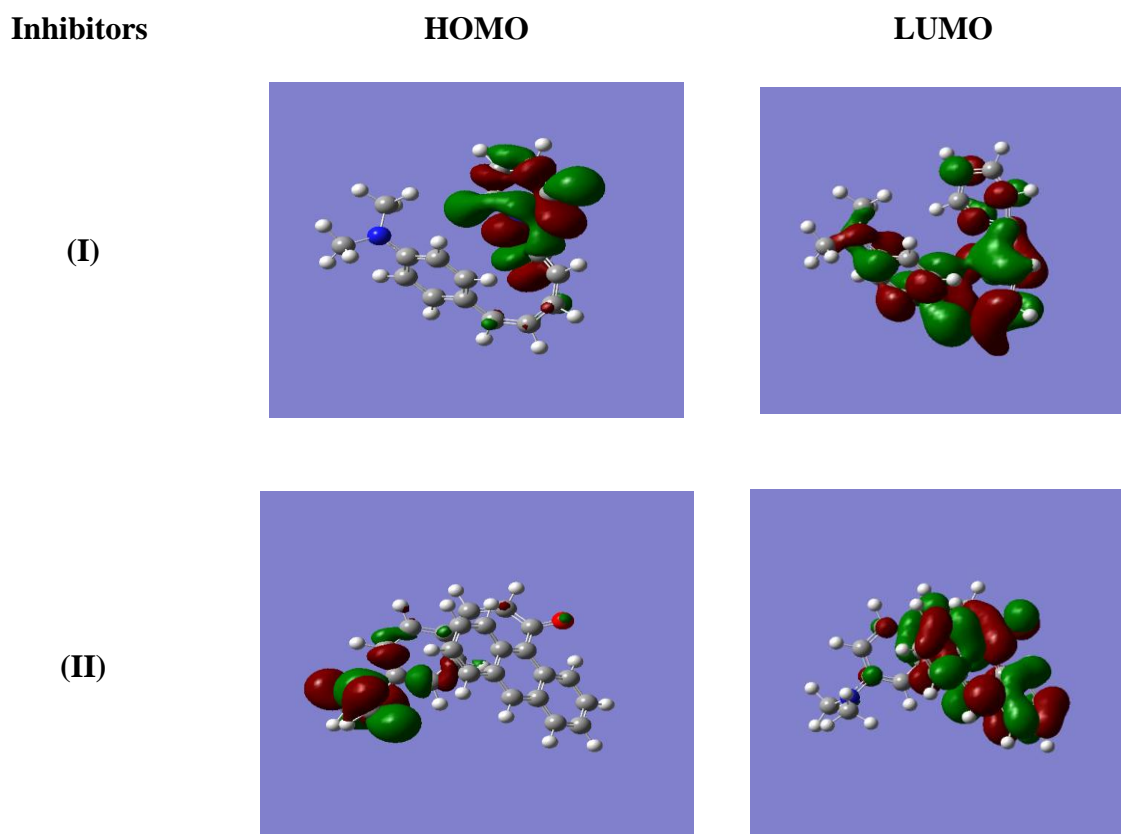


Figure 11. Molecular orbital curves of investigated dimethylamino compounds.

Table 9. The quantum calculated for investigated dimethylamino compounds.

| Factors | Compound (I) | Compound (II) |
|------------------------------|--------------|---------------|
| $-E_{\text{HOMO}}$ (a.u) | 0.23615 | 0.22783 |
| $-E_{\text{LUMO}}$ (a.u) | 0.24732 | 0.23714 |
| ΔE (a.u) | 0.016 | 0.009 |
| η (a.u) | 0.008 | 0.005 |
| σ (a.u) ⁻¹ | 126.904 | 214.823 |
| $-\text{Pi}$ (a.u) | 0.239 | 0.232 |
| χ (a.u) | 0.239 | 0.222 |

3.8. Molecular docking

Molecular docking is a key tool in computer drug design [58,59]. The focus of molecular docking is to simulate the molecular recognition process.

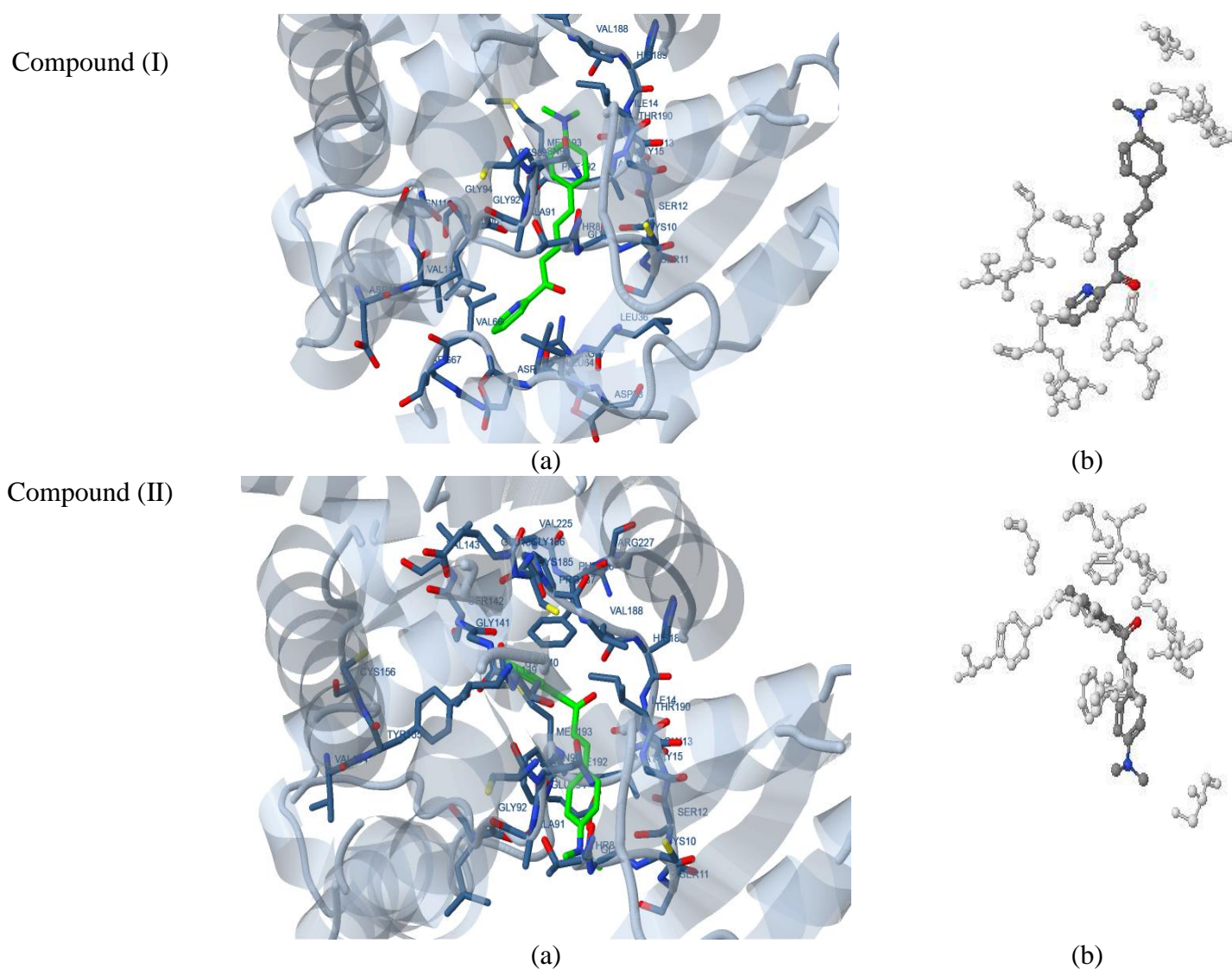


Figure 12. The organic compounds (I) and (II) (green in (a) and gray in (b)) in interaction with receptor of breast cancer mutant 3hb5-oxidoreductase.

Molecular docking aims to achieve an optimized conformation for both the protein and drug with relative orientation between them such that the free energy of the overall system is minimized. In this context, we used molecular docking between organic derivatives (I, II) and receptor of breast cancer mutant 3hb5-oxidoreductase. The results showed a possible arrangement between organic derivatives (I, II) and 3hb5 receptor. The docking study showed a favorable interaction between organic derivatives (I, II) and the receptor (3hb5) as shown in Figure. 12 and the calculated energy is listed in Table 10.

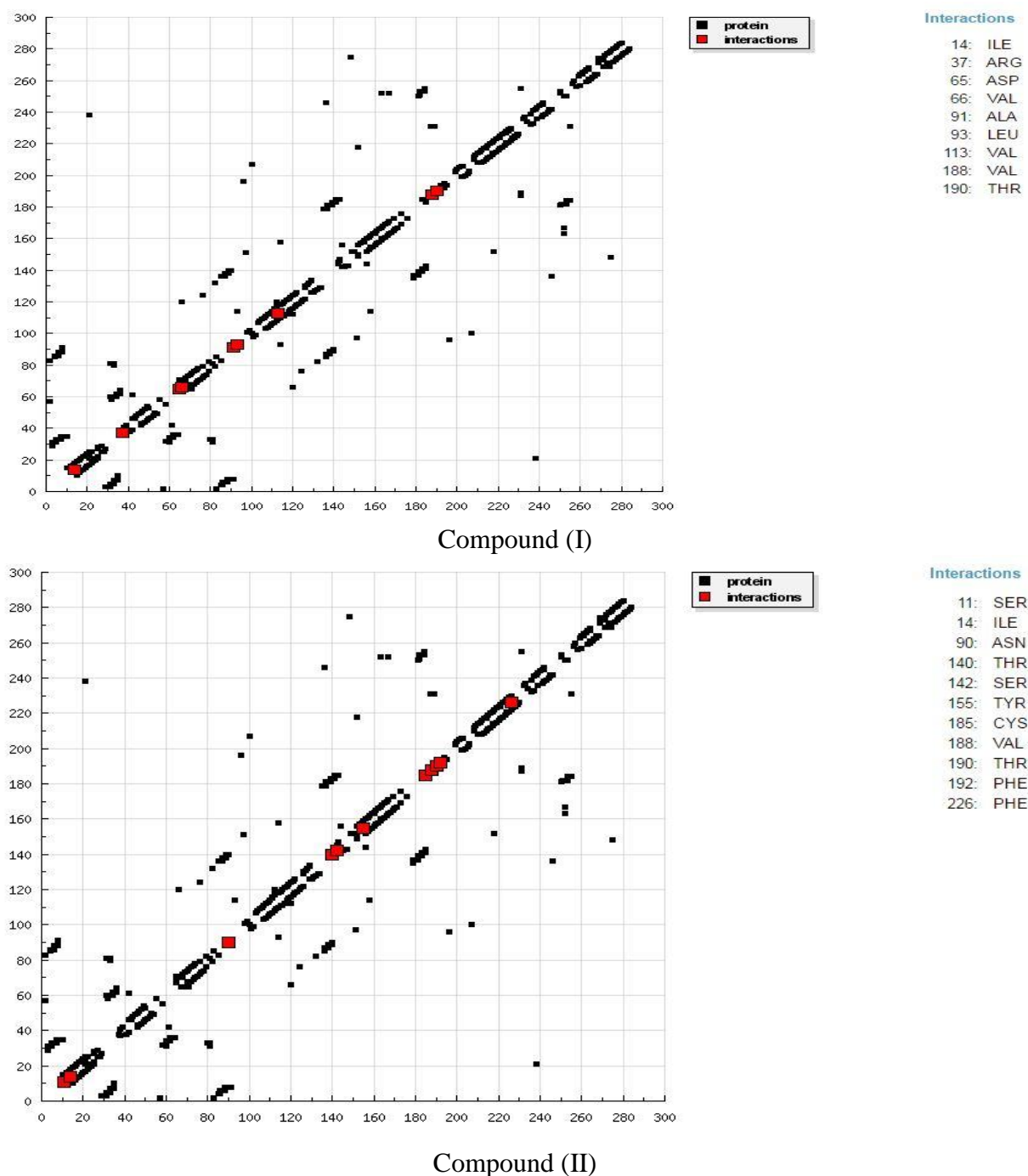


Figure 13. HB plot of interaction between compounds (I) and (II) and receptor of breast cancer mutant 3hb5-oxidoreductase.

The outcome data obtained in this paper, HB plot curve indicates that the organic (I, II) binds to the proteins with hydrogen bond interactions and decomposed interaction energies were exist among organic derivatives (I, II) with 3hb5 receptor as shown in Figure. 13. 2D plot curves of docking with organic derivatives (I, II) are shown in Figure. 14.

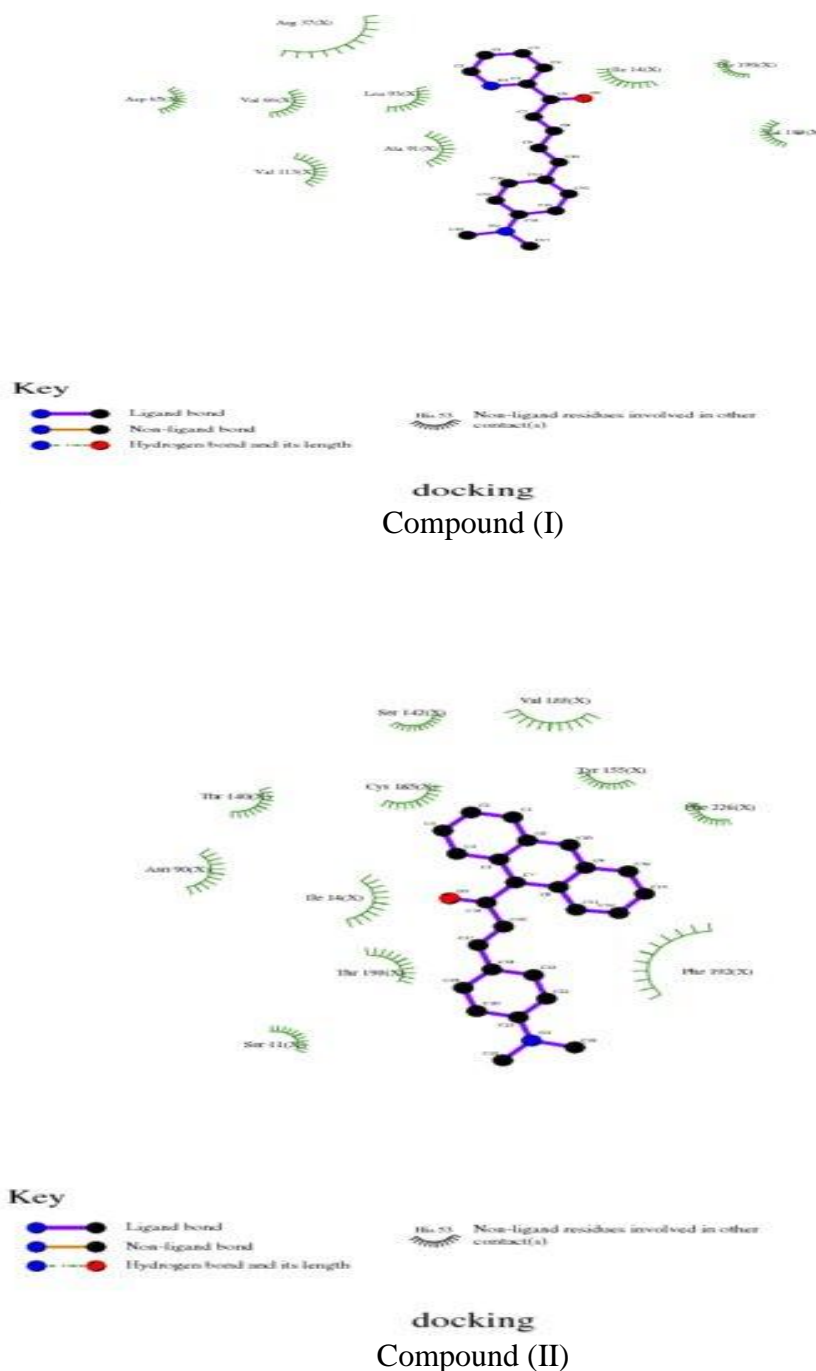


Figure 14. 2D plot of interaction between compounds (I) and (II) and receptor of breast cancer mutant 3hb5-oxidoreductase.

Table 10. Energy data given in docking evaluated of organic compounds (I, II) with receptor of breast cancer mutant 3hb5-oxidoreductase.

| Compound No. | Est. Free Energy of Binding (kcal/mol) | Est. inhibition constant (K_i) (μ M) | vdW+ bond+ desolv energy (kcal/mol) | Electrostatic Energy (kcal/mol) | Total intercooled Energy (kcal/mol) | Interact surface |
|--------------|--|---|-------------------------------------|---------------------------------|-------------------------------------|------------------|
| (I) | -6.81 | 10.11 | -8.20 | -0.09 | -8.29 | 860.085 |
| (II) | -8.42 | 672.08 | -9.58 | -0.00 | -9.58 | 955.659 |

3.9. Mechanism of Inhibition of Corrosion

The %IE depends on the kind of adsorption inhibitors on CS, metal nature, dose and surface conditions from all methods.

The outcome data of corrosion with inhibitors (I,II): The brought down of rate and i_{corr} with higher in inhibitor dose. The exchange in Tafel lines to higher potential regions. The %IE decrease with temperature rise led to desorption of the inhibitor.

It was noted that the kind of adsorption depend on the ability of the CS directly to the ring π -electron clouds. Metals for example iron, which have a stronger attract with aromatic moieties, were given to adsorb benzene rings in flat orientation.

The order of lowering IE of the composite from all method utilized is compound (II) > compound (I).

Compound (II) exhibits good power inhibition due to: (i) it has higher molecular size (351) that may facilitate best surface coverage and larger molecular area and (ii) its adsorption through two active centers (1-O , and 1-N atoms). Compound (I) comes after compound (II) in IE because it has lower molecular size (278) in spite it has three active centers (1-O and 2-N atoms).

4. CONCLUSION

1- All the investigated new eco-friendly organic derivatives are excellent corrosion inhibitors for C- steel in 2 M HCl solution. The effectiveness of these inhibitors depends on their structures. The variation in inhibitive efficiency depends on the type and the nature of the substituent present in the inhibitor molecule.

2- The adsorbed inhibitors on CS follows the isotherm Temkin

3- Double layer capacitances lower with respect to blank when the added inhibitor. This may illustrated by inhibitor adsorption on the C- steel surface.

4- The value from all tests were in agreement good. The % IE of these composites is: compound (II) > compound (I).

5- Relation among quantum calculations and IE of the investigated composite is discussed utilized the (DFT).

6- Molecular docking was utilized to predict the binding among new eco-friendly organic derivatives and the receptor of breast cancer mutant 3hb5-oxidoreductase.

References

1. M.H. Wahdan, A.A. Hermas and M.S. Morad, *J. Mater. Chem. Phys.*, 76 (2002) 111.
2. F. Bentiss, M. Lebrini, H. Vezin and M. Lagrenee, *J. Mater. Chem. Phys.*, 87 (2004) 18.
3. X. Liu, P.C. Okafor and Y.G. Zheng, *J. Corros. Sci.*, 51 (2009) 744.
4. A. Al Maofari, G. Ezznaydy, Y. Idouli, F. Guedira, S. Zaydoun, N. Labjar and S. El Hajjaji, *J. Mater. Environ. Sci.*, 5 (2014) 2081.
5. K. Barouni, A. Kassale, A. Albourine, O. Jbara, B. Hammouti and L. Bazzi, *J. Mater. Environ. Sci.*, 5 (2014) 456.
6. A.S. Fouda, K. Shalabi and H. Elmogazy, *J. Mater. Environ. Sci.*, 5 (2014) 1691.
7. A. Ostovari, S.M. Hoseinie, M. Peikari, S.R. Shadizadeh and S.J. Hashemi, *J. Corros. Sci.*, 51 (2009) 1935.
8. M.J. Bahrami, S.M.A. Hosseinia and P. Pilvar, *J. Corros. Sci.*, 52 (2010) 2793.
9. M.M. Solomon, S.A. Umoren, I.I. Udoso and A.P. Udoh, *J. Corros. Sci.*, 52 (2010) 1317.
10. H.L. Wang, R.B. Liu and J. Xin, *J. Corros. Sci.*, 46 (2004) 2455.
11. R. Solmaz, G. Kardas, B. Yazici and M. Erbil, *J. Prot. Met.*, 41 (2005) 581.
12. K.C. Emregul, R. Kurtaran and O. Atakol, *J. Corros. Sci.*, 45 (2003) 2803.
13. D. Chebabe, Z.A. Chikh, N. Hajjaji, A. Srhiri and F. Zucchi, *J. Corros. Sci.*, 45 (2003) 309.
14. F.G. Liu, M. Du, J. Zhang and M. Qiu, *J. Corros. Sci.*, 51 (2009) 102.
15. A.Y. Musa, A.A.H. Kadhum, A.B. Mohamad and M.S. Takriff, *J. Corros. Sci.*, 52 (2010) 3331.
16. K.F. Khaled and M.A. Amin, *J. Corros. Sci.*, 51 (2009) 1964.
17. M.A. Quraishi, M.Z.A. Rafiquee, S. Khan and N. Saxena, *J. Appl. Electrochem.*, 37 (2007) 1153.
18. X.Y. Zhang, F.P. Wang, Y.F. He and Y. Du, *J. Corros. Sci.*, 43 (2001) 1417.
19. M. Knag, K. Bilkova, E. Gulbrandsen, P. Carlsen and J. Sjöblöm, *Corros. Sci.*, 48 (2006) 2592.
20. L. Wang, G.J. Yin and J.G. Yin, *J. Corros. Sci.*, 43 (2001) 1197.
21. P.C. Okafor, X. Liu and Y.G. Zheng, *J. Corros. Sci.*, 51 (2009) 761.
22. J. Zhang, J.X. Liu, W.Z. Yu, Y.G. Yan, L. You and L.F. Liu, *J. Corros. Sci.*, 52 (2010) 2059.
23. T. A. Halgren, *J. Computat. Chem.*, 17 (1998) 490.
24. G.M. Morris and D.S. Goodsell, *J. Comput. Chem.*, 19 (1998) 1639.
25. R.F. Anderson, S. S. Shinde and A. Maroz, *J. Org. Biomol. Chem.*, 6 (2008) 1973.
26. A.N. Wiercinska and G. Dalmata, *J. Electrochim. Acta*, 51 (2006) 6179.
27. A. Yurt, A. Balaban, S.U. Kandemir, G. Bereket and B. Erk, *J. Mater. Chem. Phys.*, 85 (2004) 814.
28. A.Y. Etre, *J. Appl. Surf. Sci.*, 252 (2006) 8521.
29. W.J. Lorenz and F. Mansfeld, *J. Corros. Sci.*, 21 (1981) 647.
30. I.N. Putilova, S.A. Balezin and V.P. Barannik, "Metallic Corrosion Inhibitors Pergamon" Press New York, (1960).
31. K.K. Al-Neami, A.K. Mohamed, I.M. Kenawy and A.S. Fouda, *J. Monatsh. Chem.*, 126 (1995) 369.
32. E.A. Noor, *Int. J. Electrochem. Sci.*, 2 (2007) 996.
33. J. Marsh, *Advanced Organic Chemistry* 3rd ed Wiley Eastern New Delhi (1988).
34. S. Martinez and I. Stern, *J. Appl. Surf. Sci.*, 199 (2002) 83.
35. M.A. Al-Khalidi and K.Y. Al-qahtani, *J. Mater. Environ. Sci.*, 4 (5) (2013) 593.
36. J.W. Schltze and K. Wippermann, *J. Electrochim. Acta*, 32 (1987) 823.
37. D.C. Silverman and J.E. Carrico, *J. Corrosion.*, 44 (1988) 280.

38. D.D. Macdonald and M.C.H. Mckubre, "Impedance measurements in electrochemical systems" Modern Aspects of Electrochemistry, J.O'M. Bockris, B.E. Conway and R.E. White, Eds., Plenum Press, New York (1982) 61.
39. F. Mansfeld, *J. Corrosion.*, 36 (1981) 301.
40. C. Gabrielli, "Identification of Electrochemical processes by Frequency Response Analysis" Solarton Instrumentation Group, (1980).
41. M. El Achouri, S. Kertit, H.M. Gouttaya, B. Nciri, Y. Bensouda, L. Perez, M.R. Infante and K. Elkacemi, *J. Prog. Org. Coat.*, 43 (2001) 267.
42. A. Anejjar, A. Zarrouk, R. Salghi, H. Zarrok, D. Ben Hmamou, B. Hammouti, B. Elmahi and S.S. Al-Deyab, *J. Mater. Environ. Sci.*, 4 (2013) 583.
43. S.F. Mertens, C. Xhoffer, B.C. Decooman and E. Temmerman, *J. Corrosion.*, 53 (1997) 381.
44. G. TrabANELLI, C. Montecelli, V. Grassi and A. Frignani, *J. Cem. Concr. Res.*, 35 (2005) 1804.
45. A.J. Trowsdate, B. Noble, S.J. Haris, I.S.R. Gibbins, G.E. Thomson and G.C. Wood, *J. Corros. Sci.* 38 (1996) 177.
46. F.m. Reis, H.G. de Melo and I. Costa, *J. Electrochem. Acta* .,51 (2006) 1780.
47. M. Lagrenée, B. Mernari, M. Bouanis, M. Traisnel and F. Bentiss, *J. Corros. Sci.*, 44 (2002) 573.
48. E. McCafferty and N. Hackerman, *J. Electrochem. Soc.*,119 (1972) 999.
49. H. Ma, S. Chen, L. Niu, S. Zhao, S. Li and D. Li, *J. Appl. Electrochem.*, 32 (2002) 65.
50. E. Kuş and F. Mansfeld, *J. Corros. Sci.*, 48 (2006) 965.
51. G.A. Caigman, S.K. Metcalf and E.M. Holt, *J. Chem. Cryst.*, 30 (2000) 415.
52. F. Samie, J. Tidblad, V. Kucera and C. Leygraf, *J. Atmospheric Environ.*, 39 (2005) 7362.
53. R.A. Prabhu, T.V. Venkatesha, A.V. Shanbhag, G.M. Kulkarni and R.G. Kalkhambkar, *J. Corros. Sci.*, 50 (2008) 3356.
54. G. Moretti, G. Quartanone, A. Tassan and A. Zingales, *J. Wekst. Korros.*, 45(1994) 641.
55. F. Samie, J. Tidblad, V. Kucera and C. Leygraf, *J. Atmospheric Environ.*, 40 (2006) 3631.
56. I. Lukovits, K. Palfi, I. Bako and E. Kalman, *J. Corrosion* ., 53 (1997) 915.
57. P. Zhao, Q. Liang and Y Li., *J. Appl. Surf. Sci.* 252 (2005) 1596.
58. G.G. Mohamed, A.A. El-Sherif, M.A. Saad, S.E.A. El-Sawy and Sh.M. Morgan, *J. Mol. Liq.*, 223 (2016) 1311.
59. H.M. Refaat, H.A. El-Badway and Sh.M. Morgan, *J. Mol. Liq.* 220 (2016) 802.